Investigating tar formation at low pressures in wood gasification systems, applying a novel thermo-chemical simulation model

G. Boiger[1*], V. Buff[1], A.Zubiaga[1], A.Fassbind[2], P.Caels[3]

1. Zurich University of Applied Sciences, Institute of Computational Physics, Wildbachstrasse 21, 8409 Winterthur, Switzerland
2. Zurich University of Applied Sciences, Zentrum für Produktentwicklung, Lagerplatz 22, 8400 Winterthur, Switzerland
3. Aberta Nova S.A., Rua da Fonte n 5, 7570-622 Melides, Portugal
*Corresponding author, gernot.boiger@zhaw.ch

Abstract

Even-though wood gasification remains a promising technology regarding de-centralized sustainable energy supply, its main limitations, namely the issues of unsteady operation, excessive tar-formation and consequential high maintenance requirements, have never been fully overcome. In order to tackle these deficiencies and to increase the understanding of thermo-chemical wood-gas phase reaction dynamics, a numerical model has been created. After validating the simulator against comparable software, it has been applied to predict and thus understand tar-formation phenomena within a small experimental co-current gasification system. This work particularly focuses on the investigation and minimization of tar-formation phenomena within low-pressure zones (e.g. downstream of valves) at temperatures $T \leq 500K$. Model-based analysis has led to a range of recommended measures, which reduce the occurrence of tars in low-pressure zones. Said recommendations are: i) Decrease gas residence time and ii) increase temperatures in low-pressure zones; iii) Increase hydrogen to carbon ratio as well as iv) oxygen to carbon ratio in the wood gas. While measures i) and ii) require modifications to the plant and/or process itself (e.g. by installing modified pipes or by re-circulating thermal energy via heat-exchangers), measures iii) and iv) can be implemented either by removing coal from the reaction zone or by adding either water or process air to the process.

1. Introduction

The method of gasifying wood via drying, pyrolysis, reduction, consequential partial oxidation to combustible *wood-gas*, gas purification, feeding a gas motor and producing electricity via a generator, has been applied for decades. Still wood gasification remains a promising technology regarding future, de-centralized, sustainable energy supply. However, the main limitations of the technology, namely the issue of excessive tar formation and consequential high maintenance requirements, have never been fully overcome. In the course of a long term effort aiming to develop a low-tar, low-maintenance gasification device, capable of sustainably gasifying any wood-based cellulose, it has become obvious that a thorough understanding of thermo-chemical gas-phase reaction dynamics within the reactor, as well as within the gas-purification system is imperative. Thus a numeric model to account for wood-gas-phase dynamics as well as thermo-chemical equilibrium states has been considerably advanced from an original version presented in [1].

After validating the simulator based on results derived from comparable well-known thermo-dynamic solvers, it has been applied to explain, predict and thus understand tar-formation phenomena within an experimental wood-gasification plant yielding approximately 15kW of thermal- as well as approximately 3kW of electrical energy. A particular focus within this work is laid on the investigation and minimization of tar formation as well as condensation phenomena, in the light of gradually reducing temperatures as well as sudden pressure drops. Phenomena of the latter kind have been observed extensively within the mentioned experimental gasification-device, downstream of valves, bents or any gas-flow obstacles within temperature zones below 500K. These condensation events impeach the stationary function of the whole process, such that ultimately frequent maintenance stops are required. Said observations correspond to reports from other small- to large-scale gasification systems all over the world.

Model based analysis of tar condensation in low-temperature, low-pressure zones has now lead to: i) The assurance that a theoretical framework based on dynamically simulating thermo-chemical reactions thus minimizing the Gibbs Free Energy of wood-gas systems, can predict the very same qualitative increase in tar formation at low-pressures, which is observed in real-life; ii) A thorough understanding of these effects; iii) The recommendation of a range of constructive and process-based measures to reduce the occurrence of tars, in order to considerably prolong maintenance periods.

2. Concept and Methodology

Basic Modeling Concept

Based on system-dynamic principles, the newly developed wood-gas phase simulator is inspired by a unifying perspective on general physical phenomena as basically described within Gibbs Fundamental Equation (Eqn.1), where a change in global energy of any system dE is attributed to the sum of any physical potentials φ_j times the change of respectively attributed conservative quantities $d\Psi_j$, [6]. In the face of thermo-chemical investigation, the global energy change becomes a change of total Gibbs Free Energy per chemical species ΔG_i, the driving potential specializes to the species-specific molar Gibbs Free Energy $\underline{G}_i$ and the conservative property becomes the total amount of moles per chemical species N_i (Eqn.1).

$$dE = \sum_j \varphi_j d\Psi_j = dG_i = -\sum_i \underline{G}_i dN_i \qquad \text{Eqn.1}$$

In addition the local temperature T, the molar gas-phase composition x_i and local pressure p have an impact on the molar Gibbs Free Energies of each species and will cause deviations from their standard states $^{\Theta}$ (see Eqn.2).

$$\Delta\underline{G}_i\left(T,p,x_i\right) = \Delta\underline{G}_i^{\Theta}\left(T,p^{\Theta}\right) + TR\ln\left(p\cdot x_i / p^{\Theta}\right) \qquad \text{Eqn.2}$$

The knowledge of molar Gibbs Free Energies of formation in standard state $\Delta\underline{G}_i^{\Theta}$ calls for a calculation of molar standard entropies- and enthalpies of formation, which in turn require the implementation of the proper thermo-dynamic coefficients for each species. The latter were extracted from [8].

A balance of species specific molar Gibbs Free Energies with respect to stoichiometric constants γ_{ji} for species i and reaction j, is the basis for calculating prevailing molar Gibbs Free Energies of reaction $\Delta\underline{G}_{R,j}$ according Eqn. 3.

$$\Delta \underline{G}_{R,j}\left(T,p,x_i\right)=\Delta \underline{G}^{\Theta}_{R,j}\left(T,p^{\Theta}\right)+TR\sum_i \ln\left(p\cdot x_i^{\gamma_{ji}}/p^{\Theta}\right) \quad \text{Eqn. 3}$$

Any modeled chemical reaction j is driven by a non-zero molar Gibbs Free Energy of reaction and is governed in speed by approximate models based on Arrhenius Kinetics as provided in [2] and [4]. The chosen approach rather relies on relative inter-reaction-comparison than on absolute reaction rates, whereby a more detailed description is provided in [1] and [3].

Fig.1 presents a graphical interpretation as well as a very condensed and generalized version of the underlying modeling scheme. Hereby the rectangular containers represent conservative quantities Ψ_j, the filling heights of these containers are driving potentials φ_j and their cross sectional floor areas are system-capacities κ_j. In addition the arrows with solid dots are fluxes of the conservative quantities $I_{\Psi j}$, single dots are information processing units (e.g. equations) and the dashed arcs are conveyors of information. Furthermore N_{tot} and N_i are total- and species- specific amounts of molecules respectively.

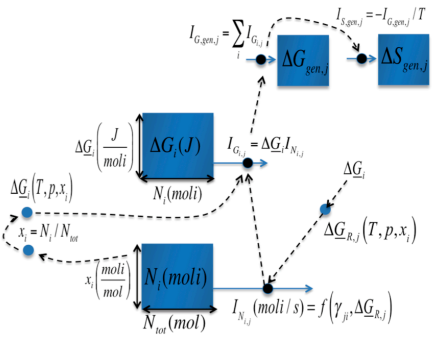

Fig.1: Graphic interpretation of the essentials of the underlying modelling scheme where i is any chemical species and j any chemical reaction.

A mathematical interpretation of the graphic solver concept within Fig.1 amounts to a series of coupled ordinary 1st order differential equations according Eqn.4 and Eqn.5, which combine with the coupling relations within Eqn.2 and Eqn.3.

$$\frac{dN_i}{dt}=\sum_j I_{N_{i,j}}\left(\gamma_{ji},\Delta \underline{G}_{R,j}\right) \quad \text{Eqn.4}$$

$$\frac{dG_i}{dt}=\sum_j I_{G_{i,j}}=\sum_j \Delta \underline{G}_i\cdot I_{N_{ij}} \quad \text{Eqn.5}$$

The differential equations are discretized with respect to time; a linear system of equations is assembled and numerically solved by a four-step Runge-Kutta scheme [9].

Chemical Species and Reactions

The simulation model considers the following interacting chemical species: coal C(s), water H_2O(g), methane CH_4(g), carbon-dioxide CO_2(g), carbon-monoxide CO(g), hydrogen H_2(g) and naphthalene $C_{10}H_8$(g). Thereby naphthalene is used to represent any tar components. The reason for choosing naphthalene, as representative for a wide range of tar-molecules, is its relatively high condensation temperature. If a gasification system is designed such that occurring naphthalene will not condensate, then it is likely that other tar components with lower condensation temperatures will not condensate either.
Within the simulation model the above mentioned chemical species interact in terms of the following chemical reactions: heterogeneous- i) Boudouard (Eqn.6), ii) Methanation (Eqn.7) and iii) Steam-Carbon (Eqn.8) reactions.

$$C(s)+CO_2 \Leftrightarrow 2CO \quad \text{Eqn.6}$$

$$C(s)+2H_2 \Leftrightarrow CH_4 \quad \text{Eqn.7}$$

$$C(s)+H_2O \Leftrightarrow CO+H_2 \quad \text{Eqn.8}$$

Those mechanisms occur in combination with a iv) variety of possible oxidation reactions, which can be summarized as seen in Eqn.9, where k, n and m are the relative stoichiometric amounts of carbon-, oxygen- and hydrogen atoms respectively.

$$C_k O_n H_m + \left(\frac{m-2n}{4} + k\right) O_2 \Leftrightarrow kCO_2 + \frac{m}{2} H_2O \quad \text{Eqn.9}$$

While the gasification-reactions cited in Eqn.6 to Eqn.9 correspond to approaches for modelling wood-gas equilibria found in standard literature (e.g. [2]), the hereby-presented model considerably extends this spectrum by a series of gas phase- as well as naphthalene reactions, namely: homogeneous- v) Steam-Carbon (Eqn.10), vi) Methanation (Eqn.11) and vii) Boudouard (Eqn.12) reactions as well as naphthalene-based viii) Methanation (Eqn.13), ix) Steam-Carbon (Eqn.14, Eqn.15) and x) CO_2/CO-conversion (Eqn.16, Eqn.17) reactions.

$$CO + H_2O \Leftrightarrow H_2 + CO_2 \quad \text{Eqn.10}$$

$$CH_4 + H_2O \Leftrightarrow 3H_2 + CO \quad \text{Eqn.11}$$

$$2CO + 2H_2 \Leftrightarrow CH_4 + CO_2 \quad \text{Eqn.12}$$

$$C_{10}H_8 + 16H_2 \Leftrightarrow 10CH_4 \quad \text{Eqn.13}$$

$$C_{10}H_8 + 10H_2O \Leftrightarrow 10CO + 14H_2 \quad \text{Eqn.14}$$

$$C_{10}H_8 + 20H_2O \Leftrightarrow 10CO_2 + 24H_2 \quad \text{Eqn.15}$$

$$C_{10}H_8 + 10CO_2 \Leftrightarrow 24CO + 4H_2O \quad \text{Eqn.16}$$

$$C_{10}H_8 + 10CO_2 \Leftrightarrow 20CO + 4H_2 \quad \text{Eqn.17}$$

Solver Validation

The solver has been validated by comparing its results to a well-known approach based on calculating chemical equilibria by minimization of global Gibbs Free Energy as well as minimizing deviations in atomic balances by the introduction and consequential minimization of a LaGrange function L (see Eqn.18), [1], [5], [7].

$$L = \sum_i \Delta G_i + \sum_j \lambda_j \sum_i (a_{i,j} N_i - b_j^0) \quad \text{Eqn.18}$$

The LaGrange function consists of two components: one expresses the sum of all Gibbs Free Energies of formation ΔG_i of all molecular species i, while the other stands for the j atomic species balances. Thereby λ_j and b^0_j are the LaGrangian Multiplier and the input rate of atomic species j respectively, $a_{i,j}$ is the number of atoms j per molecular species i and N_i is the total number of molecules per molecular species.

Fig.2 compares the results of the LaGrange approach to the hereby presented system-dynamic solver in terms of calculated tar-free homogeneous wood-gas equilibria compositions at $p=10^5$Pa, an oxygen to hydrogen ratio of $R_{O/H}= 1$ and a temperature range of $375K \leq T \leq 1350K$. It clearly shows 1:1 correspondence of the results. Additional validation has been presented in [1] and has been observed when comparing hereby-recommended measures to reduce tar in low-pressure zones (see chapter 3), with an experimental wood-gasification system.

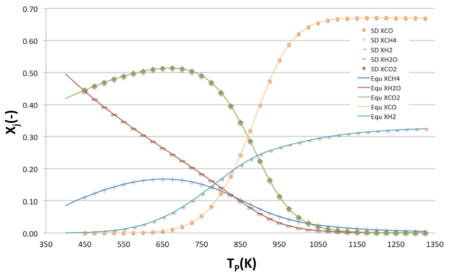

Fig.2: Wood-gas equilibria compositions x_j(-) at $p=10^5$Pa, $R_{O/H}= 1$ versus process temperature $375K \leq T_p \leq 1350K$, calculated by LaGrangian equilibrium solver ("Equ x_i") and system dynamic solver ("SD x_i").

3. Results and Discussion

Based on the, thus validated, thermo-chemical model, a dimensionless time-line of wood-gas being produced, purified and sucked towards the engine can be simulated. The solver qualitatively predicts shifts in species concentration as temperature- and pressure decrease along the wood-gas flow path. On this basis the following measures are recommended to minimize tar occurrence in low-pressure zones: i) Decrease gas residence time and ii) increase temperatures; iii) increase hydrogen to carbon ratio $R_{H/C}$ as well as iv) oxygen to carbon ratio $R_{O/C}$ in the wood gas. While measures i) and ii) require modifications to the plant- and process design itself (e.g. smaller pipes or re-circulation of thermal energy via heat-exchangers), measures iii) and iv) can be implemented by either removing coal from the reaction zone or by adding either water or process air to the process.
In the following, simulation results are presented, which lead to the recommended measures formulated above.

Measure i): Decrease gas residence time

The model does not depict chemical reaction kinetics quantitatively but qualitatively and in relative relation to each other. Still, simulations are able to show that lower-pressure can enhance naphthalene production according Eqn.13 to Eqn.17 significantly. Fig.3 demonstrates an exemplary simulation run, where lower pressures lead to faster creation of naphthalene as compared to a high-pressure case. However, the simulation-run behind Fig.3 also demonstrates that pressure differences do not necessarily have to yield a change in final equilibrium composition of naphthalene.

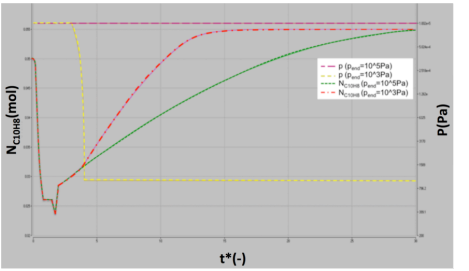

Fig. 3: Simulated absolute amount of naphthalene N_{C10H8} (mol) (case i: green; case ii: red) in wood-gas reactions versus dimensionless time t*(-), for two cases where i) pressure (purple) remains at 10^5Pa and ii) pressure (yellow) drops from 10^5Pa to 10^3Pa within dimensionless residence time window $3 \leq t^* \leq 4$. In both cases temperature drops from T=1200K to T=500K within dimensionless residence time window $1.5 \leq t^* \leq 2$. In the low-pressure case ii) (purple), naphthalene is more readily produced along the wood-gas flow path than in the high-pressure case i) (green), while the final equilibrium state remains the same in terms of naphthalene content.

On the basis of being able to simulate exemplary outcomes like this, it is fair to assume that process condition windows exist in real-life, which lead to similar effects in actual gasification systems. The obvious counter measure to avoid tar-condensation within piping systems in the context of this phenomenon is: de-crease gas residence time in critical low-pressure zones.

Measure ii): Increase temperatures

The recommendation to reduce tar condensation in low-pressure zones by increasing local temperatures does not require simulation but is an obvious counter-measure to prevent any condensation. However, increasing temperatures is just a remedy to prevent

existing tars from condensation, while measures i), iii) and iv) are meant to prevent or at least reduce tar formation itself.

Measure iii): Increase hydrogen to carbon ratio $R_{H/C}$

Selected case studies were made to simulate the effect of varying hydrogen to carbon ratios within the fuel-input (e.g. cellulose plus additives) on the naphthalene content of the wood-gas. Fig.4 shows the comparison of three simulation runs where wood-gas with varying $R_{H/C}$ ratios was exposed to temperature- and pressure drop. According to this prediction the amount of naphthalene in equilibrium decreases with increasing $R_{H/C}$. The case with the lowest $R_{H/C}$ yields highest amounts of naphthalene in the final equilibrium state. Furthermore the pressure drop causes a clearly discernable spike in naphthalene content (see $t^* \geq 4$), which points to the correspondence between calculated results and experimentally observed effects.

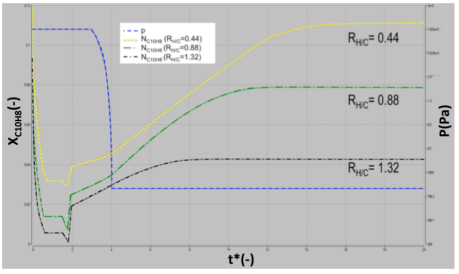

Fig. 4: Simulated relative amount of naphthalene x_{C10H8}(-) in wood-gas versus dimensionless time t*(-), for three cases where $R_{H/C}$ is set to 0.44 (yellow), 0.88 (green) and 1.32 (black) respectively, $R_{O/C}$=0.706, prescribed pressure (blue) drops from $p=10^5$Pa to $p=10^3$Pa within dimensionless residence time window $3 \leq t^* \leq 4$ and temperature drops from T=1200K to T=500K within $1.5 \leq t^* \leq 2$.

Fig.5 depicts a broader perspective on expected gas-phase compositions including naphthalene content, with increasing $R_{H/C}$. The study reveals that naphthalene content in equilibrium shows a peak at $R_{H/C} \approx 0.49$ and decreases continuously with further increase of the hydrogen to carbon ratio $R_{H/C} > 0.49$. Said peak shall hereby be referred to as *methane-emergence-threshold* since it corresponds with the appearance of methane, which is only present in equilibria compositions featuring $R_{H/C} > 0.49$. Above this threshold, additional hydrogen is apparently used rather for the formation of additional methane, than for naphthalene. Below the *methane-emergence-threshold* however, additional hydrogen will favor naphthalene formation.

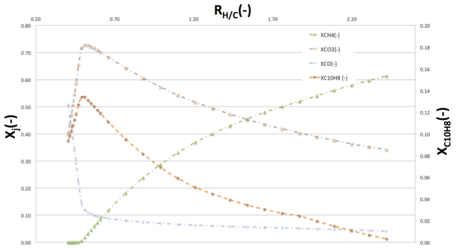

Fig. 5: Simulated wood gas equilibrium composition x_j(-) with the molar fraction of naphthalene x_{C10H8}(-) being highlighted on the right axes and with x_{H2}(-) and x_{H2O}(-) being omitted because they are below 1e-3, versus ratio of hydrogen to carbon $R_{H/C}$. In all cases ratio of oxygen-to carbon $R_{O/C}$=0.706, prescribed pressure drops from $p=10^5$Pa to $p=10^3$Pa within dimensionless residence time window $3 \leq t^* \leq 4$ and temperature drops from T=1200K to T=500K within $1.5 \leq t^* \leq 2$.

Based on these results the authors recommend the increase of $R_{H/C}$ in the gasification reactor well beyond 0.49 in order to reduce tar content in low-pressure zones. This could be achieved

e.g. by either removing coal, which would otherwise continue to participate in gasification reactions (see Eqn.6 to Eqn.8) from the reaction zone, or by adding controlled amounts of water.

Measure iv): Increase oxygen to carbon ratio $R_{O/C}$

Selected case studies were also made to simulate the effect of varying oxygen to carbon ratios within the fuel-input on naphthalene content of the wood-gas. Fig.6 shows the comparison of three simulation runs where wood-gas with varying $R_{O/C}$ ratios is exposed to temperature- and pressure drop. According to this prediction the amount of naphthalene in equilibrium decreases with increasing $R_{O/C}$. As with $R_{H/C}$ the case with the lowest $R_{O/C}$ yields highest amounts of naphthalene in the final equilibrium state.
Again the pressure drop causes a clearly discernable spike in naphthalene content, just as observed in real-life gasification systems.

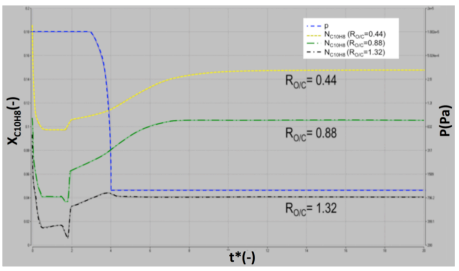

Fig. 6: Simulated relative amount of naphthalene $x_{C10H8}(-)$ in wood-gas versus dimensionless time t*(-), for three cases where $R_{O/C}$ is set to 0.44 (yellow), 0.88 (green) and 1.32 (black) respectively, $R_{H/C}$=0.706, prescribed pressure (blue) drops from $p=10^5$Pa to $p=10^3$Pa within dimensionless residence time window $3\leq t^*\leq 4$ and temperature drops from T=1200K to T=500K within $1.5\leq t^*\leq 2$.

Fig.7 depicts a broader perspective on expected gas-phase compositions including naphthalene content, with increasing $R_{O/C}$. The study shows that naphthalene content in equilibrium continuously decreases with increasing $R_{O/C}$. At $R_{O/C}\approx 0.55$ methane content reaches a minimum, causing a steeper decline in naphthalene content for $R_{O/C}>0.55$.

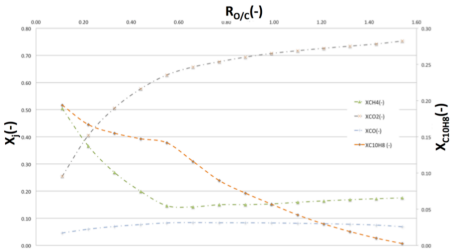

Fig. 7: Simulated wood gas equilibrium composition $x_j(-)$ with the molar fraction of naphthalene $x_{C10H8}(-)$ being highlighted on the right axes and with $x_{H2}(-)$ and $x_{H2O}(-)$ being omitted because they are below 1e-3, versus ratio of oxygen to carbon $R_{O/C}$. In all cases the ratio of hydrogen to carbon $R_{H/C}$=0.706, prescribed pressure drops from $p=10^5$Pa to $p=10^3$Pa within dimensionless residence time window $3\leq t^*\leq 4$ and temperature drops from T=1200K to T=500K within $1.5\leq t^*\leq 2$.

Based on these results, the authors recommend the increase of $R_{O/C}$ in the gasification reactor as a measure to reduce tar content in low-pressure zones. This could be achieved e.g. by either removing coal from the reaction zone, by adding more process-air, or by adding controlled amounts of water.

4. Conclusion and Outlook

This work has presented insights into the physical-, methodical- and numerical principles behind a dynamic, thermo-

chemical simulation model for the prediction of wood-gas reactions as well as compositions under conditions of varying temperatures and pressures. Besides smaller molecular species, the model includes naphthalene in order to represent the behavior of tars with high-temperature condensation points. Following its validation, the value of the software was demonstrated by deriving four concrete measures that would help to minimize tar condensation in low-pressure, low-temperature zones within real-life gasification systems. Several exemplary simulation-case studies were presented to demonstrate the existence of process-parameter windows, which would require those very measures to ensure longer maintenance intervals and smoother, tar-reduced operation of any gasification plant.

The hereby-presented dynamic thermo-chemical model is currently being converted into an easy to use, cloud-based design- and process optimization tool for wood-gasification plants. Under the name *Biogassim* and in combination with the cloud-based HPC technology *KaleidoSim*® [10], it will be free to use and accessible from anywhere in the world by the middle of 2020.

5. References

[1] G. Boiger, (2015). System Dynamic modelling approach for resolving the thermo-chemistry of wood gasification processes, (2015), Int.Journal of Multiphysics, Vol.9, (No.2), (2015), pp. 137-155;

[2] T.B. Reed, M. Markson, (2009). A Predictive Model for Stratified Downdraft Gasification, Progress in Biomass Conversion, Academic Press, New York; Vol.4, (1983), pp. 217–254;

[3] G. Boiger, (2014). A thermo fluid dynamic model of wood particle gasification and combustion processes, Institute of Computational Physics (ICP), School of Engineering, Zurich University of Applied Sciences (ZHAW), Winterthur, Switzerland, Int.Journal of Multiphysics, Vol.8, (No.2), (2014), pp. 203-230;

[4] N. Prakash, T. Karunanithi, (2008). Kinetic Modeling in Biomass Pyrolysis – A Review, Department of Chemical Engineering, Annamalai University, Annamalai Nagar. INSInet Publication, Journal of Applied Sciences Research; Vol.4, (No.12), (2008), pp. 1627-1636;

[5] S. Shabbar, I. Janajreh, (2012). Thermodynamic equilibrium analysis of coal gasification using Gibbs energy minimization method, Masdar Institute of Science and Technology (MIST), Abu Dhabi. Energy Conversion and Management; Vol.65, (2013), pp. 755-763;

[6] G. Job, F. Herrmann, (2005). Chemical potential – a quantity in search of recognition, Institut fuer Physikalische Chemie, Universitaet Hamburg, Abteilung fuer Didaktik der Physik, Universitaet Karlsruhe. European Journal of Physics; Vol.27, (2006), pp. 353-371;

[7] S. Jarungthammachote, A. Dutta, (2008). Equilibrium modeling of gasification: Gibbs free energy minimization approach and its application to spouted bed and spout – fluid bed gasifiers, Energy Field of Study, School of Environment, Resources and Development, Asian Institute of Technology, Thailand. Energy Conversion and Management, 01/2008; DOI: 10.1016/j.enconman.2008.01.006;

[8] B.J. McBride, S. Gordon, M.A. Reno, (1993). Coefficients for Calculating Thermodynamic Transport Properties, Lewis Research Center, Cleveland, Ohio, Sanford Gordon and Associates, Cleveland Ohio, Heidelberg College, Triffin, Ohio. NASA Technical Memorandum 4513, 1993;

[9] M. Hazewinkel, et.al., (2008). Runge Kutta method, Encyclopedia of Mathematics, Springer Science+Business Media B.V./Kluwer Academic Publishers; ISBN 978-1-55608-010-4, 1994;

[10] www.kaleidosim.com